

Recent advances in dye-sensitized solar cells: from photoanodes, sensitizers and electrolytes to counter electrodes

Meidan Ye², Xiaoru Wen², Mengye Wang^{1,2}, James Iocozzia¹, Nan Zhang², Changjian Lin^{2,*} and Zhiqun Lin^{1,*}

¹ School of Materials Science and Engineering, Georgia Institute of Technology, Atlanta, GA 30332, United States

² State Key Laboratory of Physical Chemistry of Solid Surfaces, Department of Chemistry, College of Chemistry and Chemical Engineering, Xiamen University, Xiamen 361005, China

Dye-sensitized solar cells (DSSCs), as low-cost photovoltaic devices compared to conventional silicon solar cells, have received widespread attention in recent years; although much work is required to reach optimal device efficiencies. This review highlights recent developments in DSSCs and their key components, including the photoanode, sensitizer, electrolyte and counter electrode.

Introduction

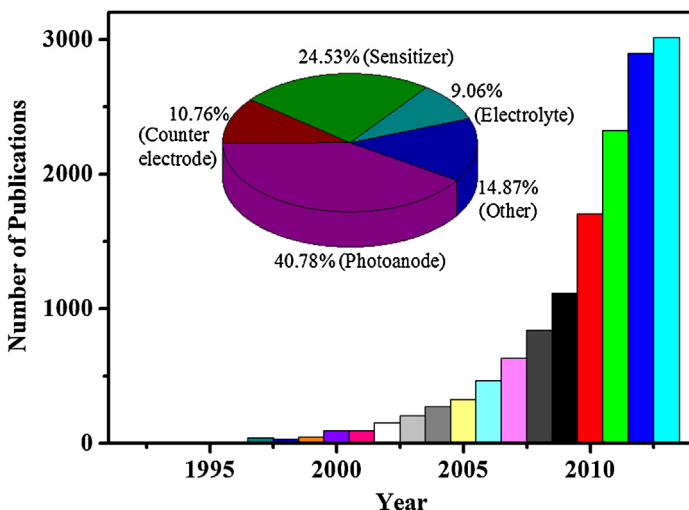
Motivated by continuously growing global energy demands and the depletion of readily accessible fossil fuels; the search for alternative energy sources, particularly renewable solar energy, has become vital. Despite the clear advantages associated with the adoption of solar cells, they need to be cost-effective and priced competitively in comparison to conventional energy resources, as any technological or performance improvements must be balanced against the associated cost [1]. Since significant breakthroughs in 1991 [2], dye-sensitized solar cells (DSSCs) have entered public view and garnered more and more research attention over the following 20 years (Fig. 1).

The most attractive properties of DSSCs are their low-cost and simple manufacturing processes together with their advantageous attributes (e.g. lightweight, flexible, low toxic, and good performance in diverse light conditions [3]). As schematically illustrated in Fig. 2, a DSSC typically consists of a several micron thick semiconductor (e.g. TiO₂, ZnO and SnO₂) film served as a photoanode that is coated or grown on a conductive substrate, a sensitizer (i.e. dye; e.g. N719, N3 or organic dyes by monolayer adsorption or quantum dots (e.g. CdS, CdSe and PbS)), an electrolyte (e.g. I₃⁻/I⁻ and Co²⁺/Co³⁺ redox couples) injected between the sensitizer and counter electrode, and a counter electrode (e.g. Pt and carbon materials) deposited on another conductive substrate [4]. Illumination by visible light irradiation on the photoanode

causes photo-excitation of the absorbed dye molecules to generate excited electrons which are subsequently injected into the conduction band of the semiconductor and quickly shuttled to the external circuit through the conductive substrate, producing an electric current. The original state of the dye is subsequently restored by electron donation from the redox electrolyte. The counter electrode returns charge from the external circuit back to the cycling circuit in the cell [4].

Each part of the device heavily determines the cost and efficiency of DSSCs. Thus, in past years almost all research effort has been focused on the modification of each component for practical applications (inset in Fig. 1). Areas of interest have included the construction of nanostructured semiconductor photoanodes with effective architectures for high dye loading and fast electron transport, the exploitation of versatile sensitizers with strong visible light harvesting ability, the utilization of redox electrolytes with useful compositions for efficient hole transport, the optimization of the Pt counter electrode as well as the development of other equivalent alternatives at lower costs [5–8]. After various attempts, a recorded power conversion efficiency (PCE) of 12.3% for liquid-electrolyte DSSCs was obtained in 2011 by using a zinc porphyrin dye YD2-o-C8 co-sensitized with another organic dye Y123, and Co^{II/III}tris(bipyridyl)-based redox electrolyte at AM 1.5 global full sun [9]. In 2013, a new milestone for solid-state mesoscopic TiO₂ solar cells sensitized with lead iodide perovskite (CH₃NH₃PbX₃) was reported to achieve an exciting power conversion efficiency of more than 15% [10–13], with expected future values as high as 20% [14].

*Corresponding authors: Lin, C. (cjlin@xmu.edu.cn), Lin, Z. (zhiqun.lin@mse.gatech.edu)

**FIGURE 1**

Evolution of the number of publications for 'sensitized solar cells'. Inset is the share distribution of publications for each component of DSSCs in 2012. Source: ISI Web of Science, Thomson Reuters.

This review highlights recent developments in the different components of DSSCs, with particular attention given to recently published works from 2011 to 2013. We will focus on the general aspects of developments. Additional information on detailed aspects can be found in special review articles with more comprehensive discussions of the photoanode, sensitizer, electrolyte and counter electrode components of DSSCs [5–8].

Recent developments in DSSC photoanodes

Nanostructured semiconductor films are the framework of DSSC photoanodes. The photoanode serves dual functions as

the support for sensitizer loading and transporter of photo-excited electrons from sensitizer to external circuit. Therefore, a large surface area is necessary to ensure high dye loading. Moreover, a fast charge transport rate is required to ensure high electron collection efficiency. These two properties are the defining characteristics of an ideal photoanode [15]. In a DSSC, a 10 µm thick film composed of a three-dimensional (3D) network of randomly dispersed spherical TiO₂ nanoparticles is typically employed as a photoanode [2]. Although the large surface area (~50 m²/g) of nanoparticles enables a high dye loading capacity, the disordered network with numerous grain boundaries weakens electron mobility and results in slow transport and recombination of photo-excited electrons. This greatly restricts the overall efficiency of such devices [16,17]. The inherent problems associated with the standard photoanode construction necessitate a search for more effective nanostructured photoanode materials and morphologies [18]. On the basis of the published literature, the recent progress in the photoanode of DSSCs can be summarized as follows.

Fabrication of various structures

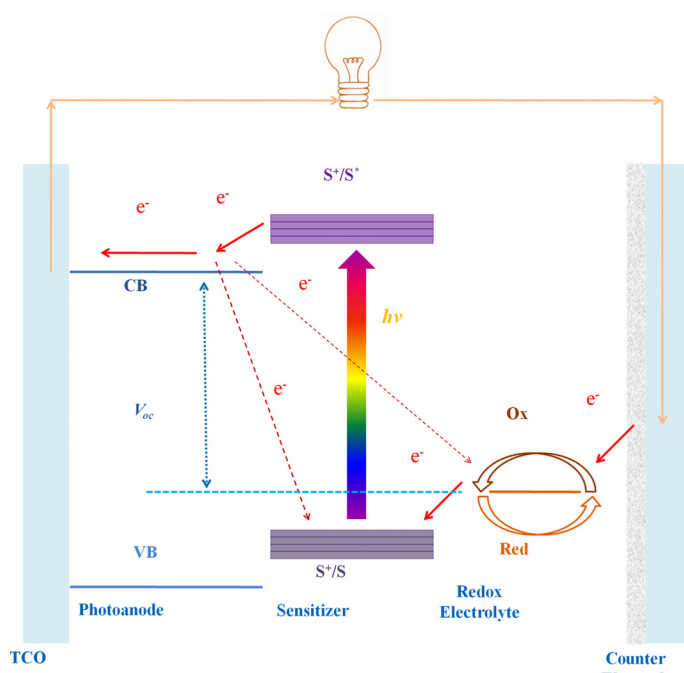
To obtain effective photoanodes, a variety of film preparation techniques, such as sol-gel [19], hydrothermal/solvothermal [20,21], electrochemical anodization [22], electrospinning [23,24], spray pyrolysis [25], and atomic layer deposition [26], have been developed and applied for crafting a diverse assortment of nanostructured semiconductor photoanodes (e.g. TiO₂, ZnO, SnO₂ and Nb₂O₅), including nanorod [27,28], nanotube [29,30], nanosheet [31], mesoporous structures [32], and 3D hierarchical architectures [33,34]. Most of these structures offer considerable efficiency improvements compared to nanoparticle systems. For example, 1D semiconductor nanostructures exhibit excellent charge transport properties [27]. Additionally, 3D mesoporous nano/microspheres, by virtue of their larger surface area (>100 m²/g), possess better light scattering properties [34].

Doping with ions

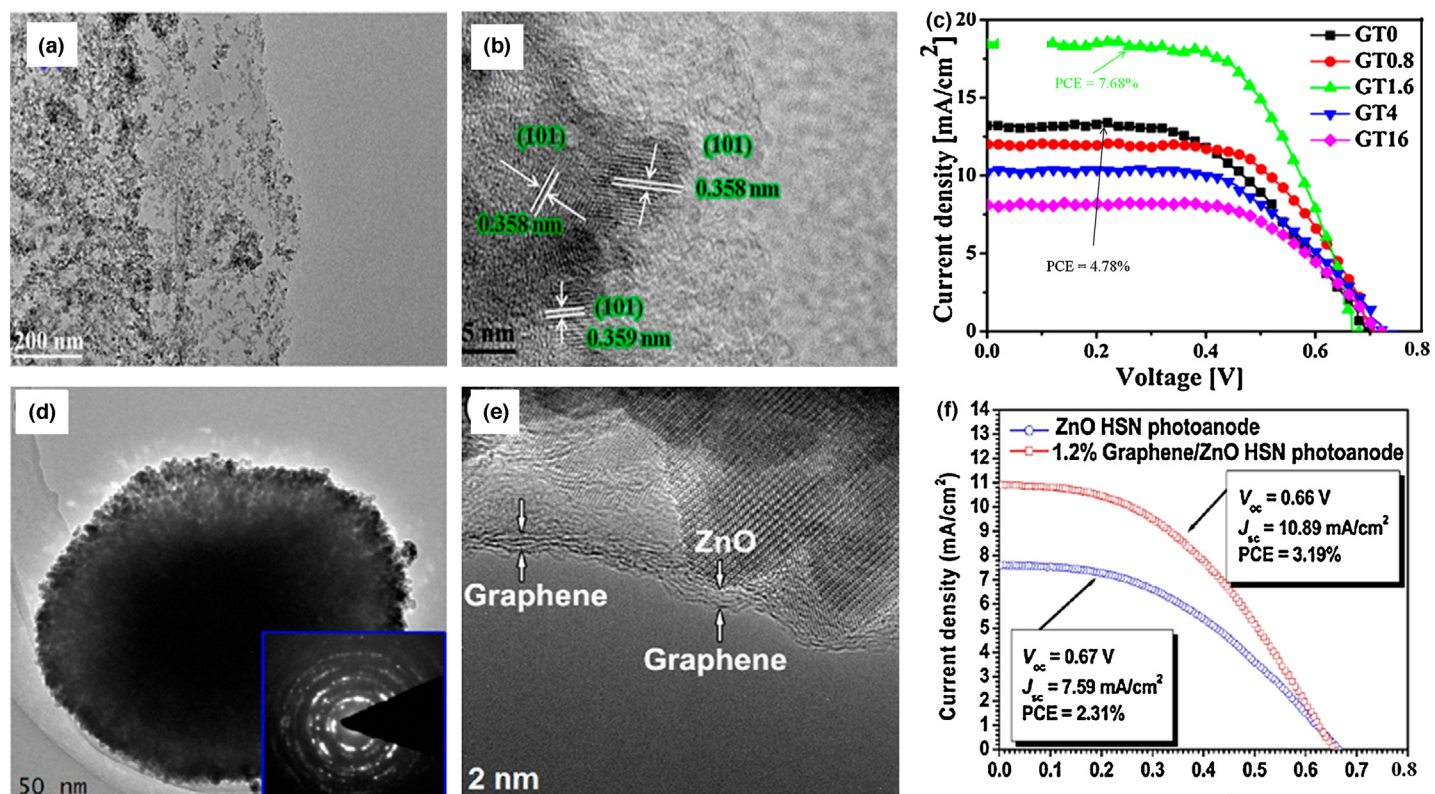
Ion doping is widely used to adjust the position of either the conduction band (CB) or valence band (VB) of semiconductor materials for photocatalysis applications. For DSSCs, ion doping (e.g. F, I, Mg, Nb and Cu) has recently been adopted to reduce recombination resistance and prolong electron lifetime in photoanodes [35–40]. However, the relevant reports are few. This is likely a consequence of the minimal impact of ion doping on DSSC efficiency as of yet.

Decoration with noble metals

The surface plasmon resonance effect (SPR) of noble metal (e.g. Au, Ag) nanoparticles has been found to localize incident light and extend the optical path length. This property has been incorporated into photoanodes to increase the light harvesting of DSSCs [41–43]. Subsequent studies have revealed that decoration with Au nanoparticles can improve electron transfer in conjunction with plasmonic and scattering effects, which are dominant over different size ranges [44]. For example, SiO₂@Ag@TiO₂ nanostructures were prepared, in which the coating of SiO₂ prevented the corrosion of Ag nanoparticles by the I⁻/I₃⁻ electrolyte and enabled enhanced light scattering and surface plasmon effect. This led to an improvement in

**FIGURE 2**

Operating principle of a dye-sensitized solar cell (DSSC). Schematic diagram of the electron-transfer processes occurring at the interfaces between each component in a DSSC.

**FIGURE 3**

TEM images of (a,b) graphene/TiO₂ and (d–e) graphene/ZnO composites. (c,f) *I*-*V* curves of the corresponding DSSCs based on graphene/TiO₂ and graphene/ZnO photoanodes. Reprinted with permission from Refs. [56,57]. Copyright 2013 American Chemical Society.

light absorption [45]. However, the effect of noble metal nanoparticles in DSSCs is still controversial and systematic investigations into their precise role are required in the future.

Modification with metal oxides

TiO₂ surface modification with an insulating layer, such as SrCO₃ [46], Al₂O₃ [47], and La₂O₃ [48], or another semiconductor layer, such as SrTiO₃ [49], SiO₂ [50], SnO₂ [51], Ga₂O₃ [52], Nb₂O₅ [53] and ZnO [54], has proven to be an effective way of increasing the efficiency of DSSCs by reducing the charge recombination in the hetero-structured photoanodes. Moreover, it has been shown that the incorporation of carbon materials (e.g. carbon nanotubes, graphene; Fig. 3) in semiconductor photoanodes facilitates transport of photogenerated electrons to ultimately enhance the DSSC performance [55–57].

Coating with up/down conversion materials

It is known that conventional sensitizers typically used in DSSCs, including ruthenium complexes and organic dyes, only absorb sunlight in the visible region. Therefore, an alternative strategy for improving and extending light-harvesting capabilities into the near-infrared region has been exploited by fabricating up-conversion nanoparticles (e.g. Yb³⁺-Tm³⁺/Yb³⁺-Ho³⁺-doped NaYF₄ and Er³⁺/Yb³⁺-doped LaF), which convert near-infrared light into visible light for the absorption of sensitizers [58,59]. Recently, some down-conversion nanocrystals, such as LaVO₄:Dy³⁺ and YF₃:Eu³⁺ were reported to down-convert ultraviolet light to visible light for increasing the current density of DSSCs [60,61]. The hetero-structured photoanodes of semiconductor-up/down conversion materials are

promising for their ability to broaden the light harvesting region of DSSCs, and thus enhance their efficiency.

Recent developments in DSSC sensitizers

The sensitizer is the central component of DSSCs because it harvests sunlight and produces photo-excited electrons at the semiconductor interface. For efficient performance, the sensitizer component has several requirements: a chemically adsorbed group to load on the semiconducting material, appropriate LUMO and HOMO levels for effective charge injection into the semiconductor and dye regeneration from the electrolyte, high molar extinction coefficients in the visible and near-infrared region for light-harvesting, good photostability and solubility, and in some cases (e.g. when cobalt-based electrolytes are used) creating the spacing between the electrolyte and photoanode to hamper the recombination [6,9]. Previously, tremendous effort has been devoted to developing a variety of sensitizers which can be divided into the following five types (Fig. 4).

Ruthenium polypyridyl dyes

As the most popular sensitizer for DSSCs, Ru(II) polypyridyl dyes show excellent performance as a result of their broad light absorption range from ultraviolet to near-infrared light ($\Delta\lambda \approx 350$ nm), suitable energy levels with respect to TiO₂ photoanodes and I⁻/I₃⁻ electrolyte, and high molecular stability [62]. Thus, as early as the mid-1990s the efficiency of Ru(II) dye-based DSSCs had already reached 10.0% [63,64], with subsequent efficiencies of 11.2% in 2005 [65], and 11.7% in 2010 [66]. Numerous recent reports still focus on the engineering of Ru(II) dyes with different ligands in

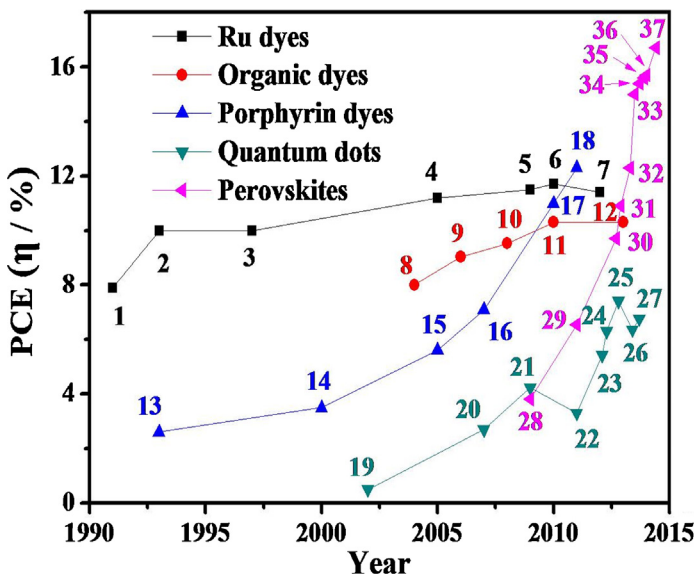


FIGURE 4

Plots of progress in PCEs of DSSC from 1991 to 2013 based on five representative sensitizers, that is, Ru dyes (1–7), organic dyes (8–12), porphyrin dyes (13–18), quantum dots (19–27), and perovskites (28–37). The labeled numbers represent different sensitizers: (1) trimeric Ru dye [2], (2) N3 [63], (3) N719 [64], (4) N719 [65], (5) CYC-B11 [72], (6) C106 [66], (7) Black dye [73], (8) Indoline dye [75], (9) D149 [76], (10) D205 [77], (11) C219 [78], (12) JF419 [79], (13) Cu-2- α -oxymesochlorin [84], (14) TCPP [87], (15) Zn-3 [85], (16) ZnTPMA-2 [86], (17) YD-2 [88], (18) YD2-oC8 [9], (19) PbS [94], (20) CdSe [91], (21) CdS/CdSe [93], (22) Sb₂S₃ [97], (23) CdS/CdSe [98], (24) Sb₂S₃ [101], (25) PbS [95], (26) CdSe_xTe_{1-x} [100], (27) CdTe/CdSe [99], (28) CH₃NH₃PbI₃ [104], (29) CH₃NH₃PbI₃ [105], (30) CH₃NH₃PbI₃ [106], (31) CH₃NH₃PbI₃Cl [107], (32) CH₃NH₃PbI_{3-x}Cl_x [108], (33) CH₃NH₃PbI₃ [10], (34) CH₃NH₃PbI_{3-x}Cl_x [12], (35) CH₃NH₃PbI_{3-x}Cl_x [13], (36) CH₃NH₃PbI₃ [11], and (37) CH₃NH₃PbI₃ [109].

order to improve overall device efficiency and stability [67]. Strategies such as incorporating functionalized ancillary ligands (e.g. triazolylpyridine and butyloxy-substitutedbenzene ring) [68,69], replacing the thiocyanate ligands with other chelating anions (e.g. cyclometalates and pyridyl azolate) [70], and featuring hydroxamate instead of carboxylate and phosphonate groups in Ru(II) dye have been investigated [71]. However, the efficiency of Ru(II) dye-based DSSCs has remained stagnant over the past ten years (Fig. 4) [72,73]. The relatively low molar extinction coefficients ($\epsilon = 10,000\text{--}20,000 \text{ M}^{-1} \text{ cm}^{-1}$) of Ru(II) polypyridyl dyes and the high cost of ruthenium have motivated investigation into new types of sensitizers.

Metal-free organic dyes

Metal-free organic dyes have also received intensive research interest as promising sensitizers in DSSCs owing to their high molar extinction coefficient ($\epsilon = 50,000\text{--}200,000 \text{ M}^{-1} \text{ cm}^{-1}$), cost-effective synthesis processes, and high flexibility of the molecule structures [74]. Consequently, a large number of organic dyes, most of which are designed with a donor-II spacer-acceptor (D-II-A) structure, have been extensively investigated for use in DSSCs (Fig. 4) [75–78]. Such organic dyes generally consist of electron-rich moieties (e.g. triarylamines, carbazoles, and indolines) as donor parts, II-conjugated groups (e.g. polyenes, thiophenes, and benzothiadiazole) as *p*-spacer parts and electron-withdrawing units (e.g. cyanoacrylic acid, rhodamines, and

pyridines) as acceptor parts [6]. To date, the best conversion efficiency of DSSCs using D-II-A type organic dyes is about 10% [78,79]. Recently, D-A-II-A and D-D-II-A type organic dyes have been developed by inserting the subordinate acceptor/donor (e.g. 2,3-diphenylquinoxaline/3,6-ditert-butylcarbazole) to facilitate electron migration, inhibit dye aggregation and improve photostability [80–82]. However, the relatively narrow absorption bands ($\Delta\lambda \approx 100\text{--}250 \text{ nm}$), adverse dye aggregation and instability represent a major bottleneck for further improvements in metal-free organic dye sensitizers.

Porphyrin dyes

In recent years, investigation into porphyrin dyes, particularly the push-pull type dipolar Zn(II) porphyrins, for DSSCs have remarkably increased because of their intense absorption in the region of 400–500 nm (Soret band, $\epsilon > 100,000 \text{ M}^{-1} \text{ cm}^{-1}$) and 500–700 nm (Q-band, $\epsilon > 20,000 \text{ M}^{-1} \text{ cm}^{-1}$), excellent molecular stability, and appropriate energy levels with versatile structures [83–87]. Porphyrin-sensitized DSSCs with the YD-2 dye attained a PCE of 11% in 2010 [88], which was further increased to 11.9% by using another porphyrin dye (YD-2-o-C8) in 2011 (Fig. 4) [9]. Several previous studies have shown that it is challenging to harvest the sunlight from the ultraviolet to near-infrared region as well as sustain efficient injection of photoexcited electrons into photoanodes using only a single porphyrin dye sensitizer [89]. Thus, co-sensitized methods have been developed as an effective method to extend the light-harvesting range and enhance DSSC efficiency. In 2011, a record breaking efficiency of 12.3% for DSSCs was obtained using YD2-oC8 co-sensitized with an organic dye (Y123) [9].

Quantum-dot sensitizer

Inorganic semiconductor quantum dots (QDs) are another material with promising use as sensitizers because of their tunable size/shape-dependent energy bandgaps, high optical absorption coefficients ($\alpha = \sim 100,000 \text{ cm}^{-1}$), large dipole moments, and multiple exciton generation characteristic [90]. The most commonly used quantum-dot sensitizers can be generally classified into three types: (a) cadmium-chalcogenide QDs, including CdS (energy bandgap, $E_g = \sim 2.25 \text{ eV}$, optical absorption edge, OAE = $\sim 550 \text{ nm}$), CdSe ($E_g = \sim 1.7 \text{ eV}$, OAE = $\sim 720 \text{ nm}$), CdTe ($E_g = \sim 1.45 \text{ eV}$, OAE = $\sim 860 \text{ nm}$) and their nanocrystal alloys [91–93]; (b) lead-chalcogenide QDs, including PbS ($E_g = 0.9\text{--}1.1 \text{ eV}$, OAE = $\sim 1300 \text{ nm}$), PbSe ($E_g = 0.7\text{--}1.7 \text{ eV}$, OAE = $\sim 1500 \text{ nm}$) [94–96]; and (c) antimony sulfide Sb₂S₃ QDs ($E_g = \sim 1.65 \text{ eV}$, OAE = $\sim 750 \text{ nm}$) [90,97]. Co-sensitization is intensively applied in cadmium-chalcogenide QD-based solar cells to reduce the charge recombination for enhanced device performance, such as CdS/CdSe (PCE = 5.42%) [93,98], CdTe/CdSe (PCE = 6.76%) [99] and CdSe_xTe_{1-x} (PCE = 6.36%) QDs (Fig. 4) [100]. Lead-chalcogenide QD-based solar cells have also been heavily studied in recent years due to their effective light harvesting in the near-infrared region and show the highest efficiency of 7.4% (Fig. 4) [95]. Sb₂S₃ may prove to be an attractive photovoltaic material because of its abundance, nontoxic elemental composition, and the high efficiency of its corresponding solar cells (6.3%) (Fig. 4) [101]. Until now, the open-circuit voltage (V_{OC}) and fill factor (FF) of QD-sensitizer solar cells (QDSSCs) are still low due primarily to the charge loss at the TiO₂/QD and TiO₂/electrolyte

interfaces. Efforts to reduce the interfacial resistance are essential for future studies.

Perovskite-based sensitizers

Recently, halide perovskite $\text{CH}_3\text{NH}_3\text{PbX}_3$ ($\text{X} = \text{Cl}, \text{Br}$, or I) sensitizers have attracted considerable attention because of their excellent light-harvesting characteristics ($E_g = \sim 1.5 \text{ eV}$, OAE = $\sim 820 \text{ nm}$, $\varepsilon = \sim 150,000 \text{ M}^{-1} \text{ cm}^{-1}$) [14, 102, 103]. In 2009, the first perovskite-sensitized solar cell was reported, showing a PCE of 3.81% for $\text{CH}_3\text{NH}_3\text{PbX}_3$ [104], which was further increased to 6.5% in 2011 [105]. Later in 2012, a major advance was obtained for $\text{CH}_3\text{NH}_3\text{PbX}_3$ -based solar cells with a maximum PCE of 9.7% [106] which was quickly raised to 10.9% [107]. In 2013, a remarkably enhanced PCE of 12.3% for perovskite $\text{CH}_3\text{NH}_3\text{PbX}_3$ -based solar cells was reported [108], which was promptly jumped to $\sim 15\%$ in the same year (Fig. 4) [11–13, 10]. Early in 2014, such PCE of perovskite $\text{CH}_3\text{NH}_3\text{PbX}_3$ -based solar cells was further lifted to 16.7% [109]. Interestingly, several researches have demonstrated that even in the absence of hole transport materials or TiO_2 films, perovskite solar cells still exhibited a high PCE of 7–8% [110, 111]. Notably, the PCE of flexible perovskite solar cells has recently been over 10% [112]. As a new type of third-generation photovoltaic device with the advantages of high efficiency, low cost, ease of manufacturing, perovskite solar cells are currently an area of intense study with PCEs of 20% expected in the near term [14].

Recent developments in DSSC electrolytes

Redox electrolytes in DSSCs function as the medium to transfer electrons from the counter electrode to the oxidized dye. The solubility and ionic mobility of a redox couple in organic medium, driving force for the dye regeneration, and fast electron transfer kinetics with a minimal overpotential at the counter electrode are crucial for an effective redox electrolyte. Furthermore, the type of electrolytes significantly impacts both the efficiency and stability of DSSCs [7, 113]. Readily classified by their physical state, electrolytes can be roughly divided into three categories: liquid electrolyte, quasi-solid electrolyte, and solid-state electrolyte.

Liquid electrolyte

As demonstrated over the past several years, the iodide-triiodide (I_3^-/I^-) electrolyte has been recognized as the most universal redox shuttle because of its satisfactory kinetic properties, such as fast oxidation of I^- at the photoanode/electrolyte interface for efficient dye regeneration and slow reduction of I_3^- at the electrolyte/counter electrode interface for high carrier collection, excellent infiltration, relative high stability, low cost and easy preparation [7]. To date, the PCE of I_3^-/I^- electrolyte-based DSSCs has been roughly 11% [66]. Despite this, several shortcomings exist for the I_3^-/I^- electrolyte. Disadvantages such as the absorption of visible light at 430 nm, corrosion of the noble metal counter electrode (e.g. Pt, Au), and an upper limit on V_{OC} of 0.9 V, significantly restrict further development of DSSCs using this electrolyte system [74]. As a result, several alternative electrolytes have been investigated, including $\text{Co}^{(\text{II}/\text{III})}$ polypyridyl complex, ferrocenium/ferrocene (Fc/Fc^+) couple, $\text{Cu}^{(\text{I}/\text{II})}$ complex, and thiolate/disulfide mediator [7]. In 2011, the $\text{Co}^{(\text{II}/\text{III})}$ polypyridyl redox couple contributed to a remarkable PCE of 12.3% for liquid

electrolyte-based DSSCs with a high V_{OC} of 0.935 V [9]. Since then, several related studies of $\text{Co}^{(\text{II}/\text{III})}$ complex electrolytes have been performed [114–117]. The slow diffusion of bulky $\text{Co}^{(\text{II}/\text{III})}$ complex into photoanode films and the fast recombination of photo-excited electrons with the oxidized redox species along with the long-term stability concerns make $\text{Co}^{(\text{II}/\text{III})}$ complex electrolytes a challenging, though possibly rewarding system to develop and improve [74].

Quasi-solid electrolyte

In the case of liquid electrolytes, sealing problems and long-term durability substantially hinder the practical application of DSSCs. Therefore, efforts have been directed toward alternatives to liquid electrolytes, that is, quasi-solid-state electrolytes and solid-state electrolytes [118]. Ionic liquids (e.g. 1-propargyl-3-methylimidazolium iodide, bis(imidazolium) iodides and 1-ethyl-1-methylpyrrolidinium) and polymer gel (e.g. poly(ethylene oxide), poly(vinylidenefluoride) and polyvinyl acetate) containing redox couples are commonly used as quasi-solid-state electrolytes to overcome the volatilization and leakage problems of liquid electrolytes [119–121]. To date, the corresponding PCEs of DSSCs based on quasi-solid-state electrolytes have reached 8–9% [120, 122]. However, because of their thermodynamic instability under high temperature, quasi-solid-state electrolytes still suffer from solvent leakage, and thus also require careful sealing treatment when used in high temperature environments [123]. Consequently, solid-state electrolytes will be the major focus for DSSC electrolyte research and industrialization in the future.

Solid-state hole transport conductor

Solid-state electrolytes, including various hole transporting materials (HTMs) have been extensively investigated as hole acceptors to replace liquid electrolytes [123]. Several inorganic *p*-type materials (e.g. CuI/CuSCN and CsSnI_3) and organic polymers (e.g. poly(3,4-ethylenedioxythiophene) (PEDOT), 2,2',7,7'-tetrakis (N,N-di-4-methoxyphenylamino)-9,9'-spirobifluorene (spiro-MeOTAD), and poly(3-hexylthiophene) (P3HT)) have been successfully used in solid-state DSSCs (SS-DSSCs) [123–125]. CuI/CuSCN HTMs possess high hole mobility. However, fast crystallization rates result in poor filling into photoanode films, and thus SS-DSSCs show relatively low PCE of $\sim 3.8\%$ [124]. CsSnI_3 , possessing high hole mobility, low cost, abundant raw materials, and low-cost processing, is another promising *p*-type semiconductor HTM. Such electrolyte-based devices have yielded a PCE of up to 10.2% for SS-DSSC in 2012 [126]. Spiro-MeOTAD is much better than other types of organic HTMs [127], and in 2013 produced a high PCE of 15% when used in perovskite-based SS-DSSCs [10]. However, low hole mobility and high manufacturing costs still inhibit the application of spiro-MeOTAD in SS-DSSCs. Good diffusion of HTMs into photoanode films and high conductivity for effective hole transfer are key issues for solid-state electrolytes in high-performance SS-DSSCs.

Recent developments in DSSC counter electrodes

The counter electrode (CE) in DSSCs has the important task of collecting electrons from the external circuit and catalyzing the reduction of redox electrolyte or transporting holes in solid-state

TABLE 1

Photovoltaic performance of DSSCs utilizing composite CEs

Counter electrode	Sensitizer	Photoanode	Electrolyte	PCE (%)	vs. Pt (%)	Ref.
Graphene-TaON	FNE29	TiO ₂	Co(bpy) ₃ ^{3+/2+}	7.65	7.91	152
Graphene-NiS₂	N719	TiO ₂	Iodide	8.55	8.15	153
Graphene-PPy	N719	TiO ₂	Iodide	5.27	6.02	154
Graphene-NiO	N719	TiO ₂	Iodide	7.42	8.18	155
CNTs-graphene	N719	TiO ₂	Iodide	8.23	7.61	132
CNTs-NiS	N719	TiO ₂	Iodide	7.90	6.36	157
CNTs-WS₂	N719	TiO ₂	Iodide	6.41	6.56	158
CNTs-PEDOT:PSS	N719	TiO ₂	Iodide	8.3	7.5	159
CNTs-TiN	N719	TiO ₂	Iodide	5.41	5.68	160
PEDOT:PSS-CuInS₂	N719	TiO ₂	Iodide	6.50	6.51	150
PEDOT:PSS-TiN	CYC-B1	TiO ₂	Iodide	6.67	6.57	161
PEDOT:PSS-CoS	N719	TiO ₂	Iodide	5.4	6.1	162

electrolyte. High conductivity for charge transport, good electrocatalytic activity for reducing the redox couple and excellent stability are the primary requirements for CE materials [74]. Noble metals, such as Pt, Au and Ag, are the most popular CE materials because of their high electrocatalytic activity (e.g. Pt) for the reduction of redox couples in liquid electrolytes or effective hole transfer in solid-state electrolytes (e.g. Au and Ag) [8]. However, noble metals are expensive and their corrosion in liquid electrolyte is a concern. Consequently, several alternatives have been extensively explored to replace noble metal CEs.

Carbon materials

Owing to their low cost, good electrocatalytic activity, high electrical conductivity, high thermal stability and corrosion resistance, carbon materials (e.g. porous carbon, carbon nanotubes (CNTs) and graphene) have been intensively used as CEs and have yielded high-performance DSSCs [128–131]. Recent studies have shown that combining two carbon materials, for example, porous carbon/carbon nanotubes [132], and carbon nanotube/graphene nano-ribbons [133], can further amplify the electrocatalytic activity of CEs. The interconnection of carbon materials and other types of CE materials is also a popular area of research.

Inorganic compounds

Sulfides (e.g. CoS₂, CuInS₂, Cu₂ZnSnS₄, Co₉S₈, Sb₂S₃, Cu₂S and CoMoS₄) [134–139], carbides (e.g. TiC) [140], nitrides (e.g. TiN, ZrN) [141,142], phosphides (e.g. Ni₂P and Ni₅P₄) [143], tellurides (e.g. CoTe and NiTe₂) [144], and metal oxides (e.g. WO₂ and V₂O₅) [145] have also been introduced as effective CE materials because of their promising application in low-cost and large-scale DSSCs. However, the performance and stability of inorganic compounds for DSSCs still need to be further improved.

Conductive polymers

Because of their high conductivity, transparency, and stability, some conductive polymers including polyaniline (PANI), poly(3,4-ethylenedioxothiophene) (PEDOT), and polypyrrole (PPy) have been employed as CE materials for DSSCs; especially for transparent and flexible DSSCs [146–148]. Among these, PEDOT is the most

commonly used CE material and doping of different components (T_{SO}⁻, ClO⁻, poly(styrenesulfonate) (PSS) and polyoxometalate (POM)) into PEDOT is frequently employed to increase its solubility and electrical conductivity in DSSCs [149,150]. Despite many available polymers to consider, cost and performance concerns remain. Further development of conductive polymer CE-based DSSCs is required.

Composites

Composite CEs, which are typically composed of two or more components that combine the merits of each component into one, have been widely investigated. In particular, composites of carbon materials and other organic/inorganic materials such as graphene-Pt/TaON/NiS₂/NiO/TiN/PPy (Table 1) [142,151–155], and carbon nanotube-Pt/TiN/NiS/WS₂/PEDOT:PSS (Table 1) have been studied [156–160]. In addition, other composites-based DSSCs, such as PEDOT:PSS-TiN/CoS/TiS₂ (Table 1) [161,162], have also shown comparable performance to devices fabricated using conventional Pt CE.

Conclusions

This review summarizes recent advances in the components of DSSCs. These include the photoanode, sensitizer, electrolyte, and counter electrode. The slow progress of DSSCs based on iodide-electrolytes and ruthenium-sensitizers in the past ten years has necessitated the need for other novel, efficient and low-cost materials for the practical commercialization of DSSCs. Thus, a series of organic/inorganic materials have been explored for the production of the cost-effective DSSCs. It is expected that a reduction in the loss-in-potential to 500 mV by well matching the energy levels at the interface of photoanode/sensitizer/electrolyte, and the further extension of the light harvesting region to 920 nm by using strongly absorbing sensitizers, the PCE of DSSCs can be boosted to 19% [62]. This is the benchmark at which such devices can compete with current thin-film photovoltaic devices. In addition to novel materials noted here, several aspects, including theoretical analysis, property characterization and device engineering are not detailed in this review but are also essential for the development of DSSCs.

Acknowledgements

M.Y. gratefully acknowledges the financial support from the Chinese Scholarship Council. This work is supported by the Air Force Office of Scientific Research (MURI FA9550-14-1-0037) (Z.L.), the National Basic Research Program of China (2012CB932900) (C.L.), and the Minjiang Scholar Program (Z.L.).

References

- [1] L. El Chaar, et al. *Renew. Sustain. Energy Rev.* 15 (2011) 2165–2175.
- [2] B. O’regan, et al. *Nature* 353 (1991) 24.
- [3] M. Gratzel, *Prog. Photovolt. Res. Appl.* 14 (2006) 429–442.
- [4] A. Hagfeldt, et al. *Chem. Rev.* 110 (2010) 6595–6663.
- [5] N. Tétreault, et al. *Energy Environ. Sci.* 5 (2012) 8506–8516.
- [6] S. Zhang, et al. *Energy Environ. Sci.* 6 (2013) 1443–1464.
- [7] M. Wang, et al. *Energy Environ. Sci.* 5 (2012) 9394–9405.
- [8] M. Wu, et al. *ChemSusChem* 5 (2012) 1343–1357.
- [9] A. Yella, et al. *Science* 334 (2011) 629–634.
- [10] J. Burschka, et al. *Nature* 499 (2013) 316–319.
- [11] D. Liu, et al. *Nat. Photonics* 8 (2013) 133–138.
- [12] M. Liu, et al. *Nature* 501 (2013) 395–398.
- [13] J.T.-W. Wang, et al. *Nano Lett.* 14 (2013) 714–720.
- [14] N.-G.J. Park, *Phys. Chem. Lett.* 4 (2013) 2423–2429.
- [15] J. Maçaira, et al. *Renew. Sustain. Energy Rev.* 27 (2013) 334–349.
- [16] X. Feng, et al. *Angew. Chem. Int. Ed.* 124 (2012) 2781–2784.
- [17] J. Wang, et al. *Chem. Asian J.* 7 (2012) 2754–2762.
- [18] S. Colodrero, et al. *Adv. Funct. Mater.* 22 (2012) 1303–1310.
- [19] A. Bahramian, *Ind. Eng. Chem. Res.* 52 (2013) 14837–14846.
- [20] H.-P. Wu, et al. *J. Phys. Chem. Lett.* 4 (2013) 1570–1577.
- [21] Z.Q. Bao, et al. *CrystEngComm* 15 (2013) 8972–8978.
- [22] N. Mir, et al. *Chem. Eur. J.* 18 (2012) 11862–11866.
- [23] H.-Y. Chen, et al. *ACS Appl. Mater. Interfaces* 5 (2013) 9205–9211.
- [24] E.N. Kumar, et al. *Energy Environ. Sci.* 5 (2012) 5401–5407.
- [25] J.H. Huo, et al. *Ind. Eng. Chem. Res.* 52 (2013) 11029–11035.
- [26] H.-J. Son, et al. *J. Am. Chem. Soc.* 135 (2013) 11529–11532.
- [27] M.Q. Lv, et al. *Energy Environ. Sci.* 6 (2013) 1615–1622.
- [28] H. Zhang, et al. *Adv. Mater.* 24 (2012) 1598–1603.
- [29] M. Ye, et al. *Adv. Mater.* 25 (2013) 3039–3044.
- [30] M.D. Ye, et al. *Nano Lett.* 11 (2011) 3214–3220.
- [31] Y. Shi, et al. *Chem. Eur. J.* 19 (2013) 282–287.
- [32] K.-N. Li, et al. *ACS Appl. Mater. Interfaces* 5 (2013) 5105–5111.
- [33] M. Ye, et al. *Small* 9 (2012) 312–321.
- [34] M. Ye, et al. *Nanoscale* 5 (2013) 6577–6583.
- [35] L. Luo, et al. *J. Power Sources* 196 (2011) 10518–10525.
- [36] J.X. Zhao, et al. *ChemPhysChem* 14 (2013) 1977–1984.
- [37] K. Mahmood, et al. *ACS Appl. Mater. Interfaces* 5 (2013) 3075–3084.
- [38] M. Stefik, et al. *ACS Nano* 7 (2013) 8981–8989.
- [39] J. Navas, et al. *Phys. Status Solidi A* 209 (2012) 378–385.
- [40] H. Pang, et al. *ACS Appl. Mater. Interfaces* 4 (2012) 6261–6265.
- [41] N. Yang, et al. *ChemSusChem* 5 (2012) 572–576.
- [42] P.-Y. Chen, et al. *ACS Nano* 7 (2013) 6563–6574.
- [43] F.P. García de Arquer, et al. *ACS Nano* 7 (2013) 3581–3588.
- [44] Q. Wang, et al. *J. Mater. Chem. A* 1 (2013) 13524–13531.
- [45] S.H. Hwang, et al. *Chem. Eur. J.* 19 (2013) 13120–13126.
- [46] S. Wang, et al. *Phys. Chem. Chem. Phys.* 14 (2012) 816–822.
- [47] X. Gao, et al. *Nanoscale* 5 (2013) 10438–10446.
- [48] H. Yu, et al. *ACS Appl. Mater. Interfaces* 4 (2012) 1289–1294.
- [49] C.W. Kim, et al. *J. Mater. Chem. A* 1 (2013) 11820–11827.
- [50] J.T.-W. Wang, et al. *Nano Lett.* 14 (2013) 714–720.
- [51] U.V. Desai, et al. *J. Phys. Chem. C* 117 (2013) 3232–3239.
- [52] A.K. Chandiran, et al. *Nano Lett.* 12 (2012) 3941–3947.
- [53] H.-N. Kim, et al. *ACS Appl. Mater. Interfaces* 4 (2012) 5821–5825.
- [54] K.S. Kim, et al. *Adv. Mater.* 24 (2012) 792–798.
- [55] K.T. Dembele, et al. *J. Phys. Chem. C* 117 (2013) 14510–14517.
- [56] G. Cheng, et al. *ACS Appl. Mater. Interfaces* 5 (2013) 6635–6642.
- [57] F. Xu, et al. *J. Phys. Chem. C* 117 (2013) 8619–8627.
- [58] J. Chang, et al. *Adv. Funct. Mater.* 23 (2013) 5910–5915.
- [59] J. Yu, et al. *J. Power Sources* 243 (2013) 436–443.
- [60] J. Wu, et al. *Sci. Rep.* 3 (2013) 631.
- [61] Z. Chamanzadeh, et al. *J. Lumin.* 135 (2013) 66–73.
- [62] B.E. Hardin, et al. *Nat. Photonics* 6 (2012) 162–169.
- [63] M.K. Nazeeruddin, et al. *J. Am. Chem. Soc.* 115 (1993) 6382–6390.
- [64] C.J. Barbe, et al. *J. Am. Ceram. Soc.* 80 (1997) 3157–3171.
- [65] M.K. Nazeeruddin, et al. *J. Am. Chem. Soc.* 127 (2005) 16835–16847.
- [66] Q. Yu, et al. *ACS Nano* 4 (2010) 6032–6038.
- [67] S.H. Park, et al. *Adv. Energy Mater.* 2 (2012) 219–224.
- [68] I. Stengel, et al. *Adv. Energy Mater.* 2 (2012) 1004–1012.
- [69] W.-K. Huang, et al. *J. Phys. Chem. C* 117 (2013) 2059–2065.
- [70] S.-W. Wang, et al. *Chem. Sci.* 4 (2013) 2423–2433.
- [71] T.P. Brewster, et al. *Inorg. Chem.* 52 (2013) 6752–6764.
- [72] C.-Y. Chen, et al. *ACS Nano* 3 (2009) 3103–3109.
- [73] L. Han, et al. *Energy Environ. Sci.* 5 (2012) 6057–6060.
- [74] Y.-S. Yen, et al. *J. Mater. Chem.* 22 (2012) 8734–8747.
- [75] T. Horiuchi, et al. *J. Am. Chem. Soc.* 126 (2004) 12218–12219.
- [76] S. Ito, et al. *Adv. Mater.* 18 (2006) 1202–1205.
- [77] S. Ito, et al. *Chem. Commun.* (2008) 5194–5196.
- [78] W. Zeng, et al. *Chem. Mater.* 22 (2010) 1915–1925.
- [79] A. Yella, et al. *Chem. Mater.* 25 (2013) 2733–2739.
- [80] S. Qu, et al. *Chem. Commun.* 48 (2012) 6972–6974.
- [81] Y. Wu, et al. *Energy Environ. Sci.* 5 (2012) 8261–8272.
- [82] S. Namuangruk, et al. *J. Phys. Chem. C* 116 (2012) 25653–25663.
- [83] L.-L. Li, et al. *Chem. Soc. Rev.* 42 (2013) 291–304.
- [84] A. Kay, et al. *J. Phys. Chem. Lett.* 97 (1993) 6272–6277.
- [85] Q. Wang, et al. *J. Phys. Chem. B* 109 (2005) 15397–15409.
- [86] W.M. Campbell, et al. *J. Phys. Chem. C* 111 (2007) 11760–11762.
- [87] S. Cherian, et al. *J. Phys. Chem. B* 104 (2000) 3624–3629.
- [88] T. Bessho, et al. *Angew. Chem. Int. Ed.* 49 (2010) 6646–6649.
- [89] M. Kimura, et al. *Angew. Chem. Int. Ed.* 51 (2012) 4371–4374.
- [90] J.H. Rhee, et al. *NPG Asia Mater.* 5 (2013) e68.
- [91] L.J. Diguna, et al. *Appl. Phys. Lett.* 91 (2007).
- [92] H.C. Chen, et al. *Adv. Mater.* 23 (2011) 5451–5455.
- [93] Y.L. Lee, et al. *Adv. Funct. Mater.* 19 (2009) 604–609.
- [94] R. Plass, et al. *J. Phys. Chem. B* 106 (2002) 7578–7580.
- [95] A.H. Ip, et al. *Nat. Nanotechnol.* 7 (2012) 577–582.
- [96] N.s. Guijarro, et al. *J. Phys. Chem. Lett.* 3 (2012) 3367–3372.
- [97] S.H. Im, et al. *Energy Environ. Sci.* 4 (2011) 2799–2802.
- [98] P.K. Santra, et al. *J. Am. Chem. Soc.* 134 (2012) 2508–2511.
- [99] J. Wang, et al. *J. Am. Chem. Soc.* 135 (2013) 15913–15922.
- [100] Z. Pan, et al. *ACS Nano* 7 (2013) 5215–5222.
- [101] J.A. Chang, et al. *Nano Lett.* 12 (2012) 1863–1867.
- [102] G. Hodes, *Science* 342 (2013) 317–318.
- [103] J.J. Bisquert, *Phys. Chem. Lett.* 4 (2013) 2597–2598.
- [104] A. Kojima, et al. *J. Am. Chem. Soc.* 131 (2009) 6050–6051.
- [105] J.-H. Im, et al. *Nanoscale* 3 (2011) 4088–4093.
- [106] H.-S. Kim, et al. *Sci. Rep.* 2 (2012) 591.
- [107] M.M. Lee, et al. *Science* 338 (2012) 643–647.
- [108] J.M. Ball, et al. *Energy Environ. Sci.* 6 (2013) 1739–1743.
- [109] N.J. Jeon, et al. *J. Am. Chem. Soc.* 136 (2014) 7837–7840.
- [110] W.A. Laban, et al. *Energy Environ. Sci.* 6 (2013) 3249–3253.
- [111] M.J. Carnie, et al. *Chem. Commun.* 49 (2013) 7893–7895.
- [112] D. Liu, et al. *Nat. Photonics* 8 (2013) 133–138.
- [113] C. Grätzel, et al. *Mater. Today* 16 (2013) 11–18.
- [114] J.-H. Yum, et al. *Nat. Commun.* 3 (2012) 631.
- [115] M.K. Kashif, et al. *J. Am. Chem. Soc.* 134 (2012) 16646–16653.
- [116] M.K. Kashif, et al. *Angew. Chem. Int. Ed.* 125 (2013) 5637–5641.
- [117] E. Mosconi, et al. *J. Am. Chem. Soc.* 134 (2012) 19438–19453.
- [118] J.N. de Freitas, et al. *J. Mater. Chem.* 19 (2009) 5279–5294.
- [119] S. Bai, et al. *ACS Appl. Mater. Interfaces* 5 (2013) 3356–3361.
- [120] M.B. Achari, et al. *Phys. Chem. Chem. Phys.* 15 (2013) 17419–17425.
- [121] L. Wang, et al. *ACS Sustain. Chem. Eng.* 1 (2012) 205–208.
- [122] X. Wang, et al. *ACS Appl. Mater. Interfaces* 5 (2012) 444–450.
- [123] D. Li, et al. *Energy Environ. Sci.* 2 (2009) 283–291.
- [124] G. Hodes, et al. *Acc. Chem. Res.* 45 (2012) 705–713.
- [125] D. Bi, et al. *J. Phys. Chem. Lett.* 4 (2013) 1532–1536.
- [126] I. Chung, et al. *Nature* 485 (2012) 486–489.
- [127] J.H. Heo, et al. *Nat. Photonics* 7 (2013) 486–491.
- [128] S.-Q. Fan, et al. *Langmuir* 26 (2010) 13644–13649.
- [129] X. Mei, et al. *Nanotechnology* 21 (2010) 395202.
- [130] H. Wang, et al. *Angew. Chem. Int. Ed.* 125 (2013) 9380–9384.
- [131] L. Kavan, et al. *Nano Lett.* 11 (2011) 5501–5506.
- [132] Y. Jo, et al. *Chem. Commun.* 48 (2012) 8057–8059.
- [133] Z. Yang, et al. *Angew. Chem. Int. Ed.* 52 (2013) 3996–3999.
- [134] M.S. Faber, et al. *J. Phys. Chem. Lett.* 4 (2013) 1843–1849.
- [135] S.-H. Chang, et al. *ACS Nano* 7 (2013) 9443–9451.

- [136] R.-Y. Yao, et al. *ACS Appl. Mater. Interfaces* 5 (2013) 3143–3148.
- [137] S.J. Yuan, et al. *Chem. Eur. J.* 19 (2013) 10107–10110.
- [138] H. Zhang, et al. *J. Phys. Chem. C* 117 (2013) 10285–10290.
- [139] X. Zheng, et al. *Chem. Commun.* 49 (2013) 9645–9647.
- [140] Y. Zhao, et al. *Nanoscale* 5 (2013) 11742–11747.
- [141] W. Wei, et al. *J. Mater. Chem. A* 1 (2013) 14350–14357.
- [142] Z. Wen, et al. *Adv. Mater.* 23 (2011) 5445–5450.
- [143] M.-S. Wu, et al. *Chem. Commun.* 49 (2013) 10971–10973.
- [144] J. Guo, et al. *Chem. Commun.* 49 (2013) 10157–10159.
- [145] M. Wu, et al. *Chem. Commun.* 47 (2011) 4535–4537.
- [146] R. Trevisan, et al. *Adv. Energy Mater.* 1 (2011) 781–784.
- [147] J. Xia, et al. *J. Mater. Chem.* 21 (2011) 4644–4649.
- [148] W. Sun, et al. *J. Mater. Chem. A* 1 (2013) 2762–2768.
- [149] C. Yuan, et al. *Ind. Eng. Chem. Res.* 52 (2013) 6694–6703.
- [150] Z. Zhang, et al. *ACS Appl. Mater. Interfaces* 4 (2012) 6242–6246.
- [151] R. Bajpai, et al. *ACS Appl. Mater. Interfaces* 3 (2011) 3884–3889.
- [152] Y. Li, et al. *ACS Appl. Mater. Interfaces* 5 (2013) 8217–8224.
- [153] Z. Li, et al. *J. Phys. Chem. C* 117 (2013) 6561–6566.
- [154] L. Chen, et al. *ACS Appl. Mater. Interfaces* 5 (2013) 2047–2052.
- [155] V.-D. Dao, et al. *Nanoscale* 6 (2014) 477–482.
- [156] H.Y. Chen, et al. *Chem. Asian J.* 7 (2012) 1795–1802.
- [157] Y. Xiao, et al. *J. Mater. Chem. A* 1 (2013) 13885–13889.
- [158] G. Yue, et al. *Carbon* 55 (2013) 1–9.
- [159] G. Guan, et al. *J. Mater. Chem. A* 1 (2013) 13268–13273.
- [160] G.-R. Li, et al. *Angew. Chem. Int. Ed.* 49 (2010) 3653–3656.
- [161] M.-H. Yeh, et al. *J. Mater. Chem.* 21 (2011) 19021–19029.
- [162] P. Sudhagar, et al. *ACS Appl. Mater. Interfaces* 3 (2011) 1838–1843.